Rapid Inertial Reorientation of an Aerial Insect-sized Robot Using a Piezo-actuated Tail

Avinash Singh[1], Thomas Libby[2], Sawyer B Fuller[1]

***Abstract*— We present the design, fabrication, and feedforward control of a insect-sized (142 mg) aerial robot that is equipped with a bio-inspired inertial tail. A tail allows the robot to perform rapid inertial reorientation as well as to shift weight to modulate aerodynamic torques on its body. Here we present the first analysis of inertial reorientation using a piezo actuator, departing from previous work to date that has focused exclusively on actuation by DC electric motor. The primary difference is that unlike a geared motor system, the piezo-tail system operates as a resonant system, exhibiting slowly-decaying oscillations. We present a dynamic model of piezo-driven inertial reorientation, along with an open-loop feedforward controller that reduces excitation of the resonant mode. We validate our approach on a tethered testbed as well as a flight-capable prototype. Our results indicate that incorporating a tail can allow for more rapid dynamic maneuvers and could stabilize the robot during flight.**

I. INTRODUCTION

The motivation to create small agile, maneuverable and capable robots approximately the size of a honeybee ($\sim$100 mg) is driven by the engineering challenges associated with miniaturization and their potential for improved performance on robotic tasks that benefit from small size. Recent advancements have included controlled flight [1] and wireless flight [2].

Given that these advancements provide evidence that robots are technically feasible, our interest in this work is in exploring the limits of their performance. Insect-sized robots are capable of rapid, dynamic maneuvers. In [3], a honeybee-sized robot demonstrated angular accelerations of nearly 20,000 deg/s^2. This compares favorably with the 10,000 deg/s^2 that was achieved by a larger, 0.5 kg quadrotor-style helicopter performing flips [4]. We hypothesize that inertial reorientation could push agility even further without sacrificing robustness.

Here we consider using an actuated, weighted appendage for Inertial Reorientation (IR) [5] to improve agility. IR is defined as control of body orientation through inertial forces that arise from internal configuration changes. Recent developments in robotic IR include aerial reorientation [6], precise and rapid yaw changes [7], rapid turns [8], [9], dynamic self righting [10], disturbance rejection [11], [12], pitch control in mid air during a jump [13]. Inertial appendages have also been applied in thrust redirection [14]. These robots have been inspired by a variety of animal morphologies including lizards [15], [16] and moths [17], [18].

[1]Department of Mechanical Engineering, University of Washington, Seattle, WA 98105, USA

[2]Department of Electrical Engineering, University of Washington, Seattle, WA 98105, USA

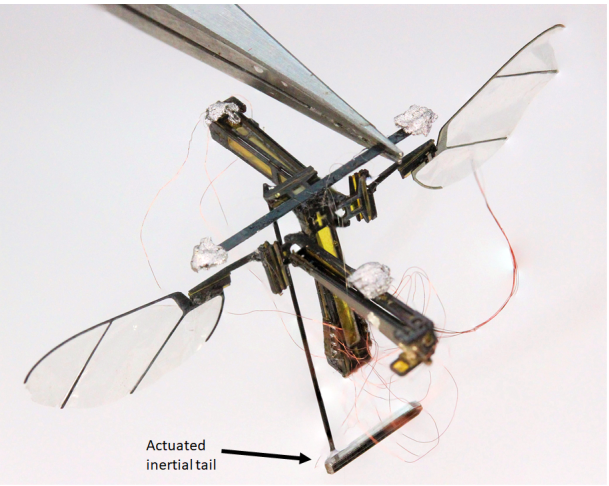

Fig. 1. Honeybee-sized flying robot equipped with a piezo-actuated tail.

In previous robot work, the appendage was actuated by a DC electric motor. As scale reduces to that of a honeybee-sized insect, however, electric motors are significantly outperformed in terms of bandwidth, efficiency, and power density by piezoelectric bimorph cantilever actuators [19], [20]. Accordingly, we are concerned in this report with adapting existing principles for inertial reorientation to the distinct properties of this technology.

The piezo actuator is combined with a specially designed transmission, emulating a four-bar kinematic chain [21] to magnify actuator displacement. The transmission amplifies a $\sim$500 μm tip motion into 70°–120° angular movement of the wing or tail. As with the actuator-wing system, the actuator-tail system is a resonant system. This characteristic is used productively in the wing system to amplify wing motion near the resonant frequency of the flapping wings, which is around 150 Hz. However, when actuating a tail, the same resonance results in undesirable oscillations with a long decay time. As part of our work we propose a solution that includes a means to construct a dynamic model that permits feedforward cancellation of these oscillations. Although passive tails have been implemented on running [22] and flying [23] microrobots, to our knowledge this work represents the first piezo-actuated tail reorientation system, and the first insect-sized robot to be equipped with an active *inertial* tail.

In this work, we adapt previous models of DC motor-actuated models of inertial reorientation to predict behavior of a piezo-based approach. We build two robots: a flight-capable prototype with an offset tail (Fig. 1), and a teth-

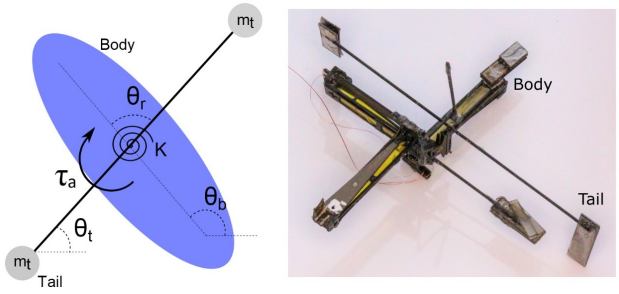

Fig. 2. A template model (left) for piezo-driven inertial reorientation and a wingless tethered testbed (right). Unlike the flight prototype in Fig. 1, both model and testbed are designed so that centers of mass of both body and tail are (approximately) coincident with the actuated joint.

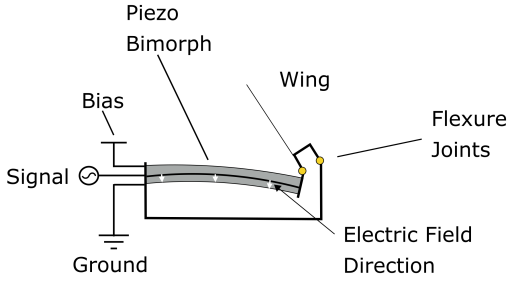

Fig. 3. Piezoelectric cantilever actuation for appendages. A microfabricated flexure transmission amplifies small tip motion generated by the reverse piezoelectric effect, resulting in large angular deflections of a wing or tail.

ered testbed with a radially symmetric tail designed to test actuator dynamics (Fig. 2). We then investigate the use of prefiltered feedforward inputs to control the tails of these robots. The paper is arranged as follows. Section II describes introduces models of the robot and its actuator, Section III describes the robot design, Section IV describes how the robot was fabricated, Section V provides the results including open loop experiments, and we conclude in Section VI.

II. MODELING AND ANALYSIS

Previous work on aerial inertial reorientation analyzed a number of candidate morphologies, including tails and flywheels [5]; we will leverage these models to design the robots discussed in this paper. The simplest and most analytically tractable of these models (known as a *Template* [24]) consists of two rigid bodies, with a joint coincident with their centers of mass (CM). This model was analyzed to provide a concise relationship between body design and performance, but utilized a DC motor-like model to constrain reorientation time. Here, we will redesign the template with a piezo-like motor model, and derive a new controller to achieve reorientation. We will use this model to design two prototypes, one that hews closely to the template for simple analysis, and another with an offset tail that enables better flight performance.

A. Actuator Behavior

As it is central to the analysis in this paper, we start with the operation of the piezo actuator. A diagram of how it operates to drive a wing or tail is given in Fig. 3. The piezo cantilever consists of a carbon fiber layer sandwiched between top and bottom layers of the piezo ceramic material. The top and bottom surface of each piezo sheet are coated with a thin conductor so that the electric potential is the same across the sheet. To drive the piezoelectric actuator, the top piezo layer is given a constant positive bias voltage (+250V) and the bottom piezoelectric layer is grounded (0V). To drive motion, the middle carbon fiber layer is given a signal voltage somewhere been these two extremes. As a result of the piezoelectric effect, the piezo material deforms in approximate proportion to the strength of the electric field, resulting in a force at the tip of the cantilever. The cantilever configuration amplifies the small piezoelectric strain, and the transmission amplifies it still further.

A piezoelectric actuator in tandem with a motion-amplifying transmission differs from a DC motor because of the lack of strong speed sensitivity of force (in comparison to the high back-emf effect of a geared DC motor). Further, the cantilevered actuator undergoes elastic bending when the output moves, adding passive stiffness parallel to actuator force. Flexures in the transmission add additional stiffness. Under the three assumptions mentioned in [21], namely, operation of the actuator with an ideal voltage source, operation of the actuator with a frequency much lower than its self-resonant frequency, and assuming negligible aerodynamic drag, the piezoelectric actuator can be assumed to behave linearly. This allows us to assume that there is a linear relation between torque applied and input voltage.

For an appendage with angle θ_r, driven by the the piezoelectric actuator through a linkage, the simplest model of the torque applied to the appendage is:

$$\tau_a = -\rho V - K\theta_r \tag{1}$$

where K is the rotational spring constant of the actuator-transmission system and ρ is a constant that relates applied voltage V to actuator torque on the tail. Here, positive voltage rotates the appendage clockwise in Fig. 2. We identify both ρ and K empirically, as described in sections IV.

B. A Piezo-driven Inertial Reorientation Template

This section adapts the Inertial Reorientation (IR) Template [5] to a piezo-like actuator model. The template in Fig. 2 is defined as a planar system consisting of two bodies, the "body" and the appendage or "tail." The two bodies are connected by a hinge modeled as a pin joint at located at their common center of mass. The actuator applies a torque τ_a on the tail, and an equal and opposite torque on the body (the orientation of which is denoted θ_b). The template is assumed to be falling or floating in space with no external forces, so that angular momentum about the CM is conserved.

Libby *et. al* [5] defined *Inertial Effectiveness* of the IR system as a dimensionless constant, ξ, which is the ratio of the tail moment of inertia (MOI) I_t, normalized by the sum

of the body MOI (I_b) and the tail MOI,

$$\xi = \frac{I_t}{I_b + I_t} \tag{2}$$

The inertial effectiveness characterizes the ratio of body velocity to relative appendage velocity for the template under zero-angular momentum reorientation. Defining an initial condition, $\theta_b(0) = \theta_r(0) = 0$, ξ kinematically relates the body angle to the relative angle,

$$\theta_b = -\xi\,\theta_r \tag{3}$$

The dynamics of the body follow from Euler's law, $I_b\ddot{\theta} = -\tau_a$ (the torque applied to the body is equal and opposite to that applied to the appendage). Plugging in the actuator model, Eqn. 1, the dynamics are,

$$I_b\ddot{\theta}_b = \rho V + K\theta_r \tag{4}$$

Since body angle is related to relative angle by (3), Eqn. (4) can be rewritten exclusively in terms of the body orientation, θ_b, so that the relative angle θ_r disappears,

$$\ddot{\theta}_b = \frac{\rho V}{I_b} - \frac{K}{\xi I_b}\theta_b. \tag{5}$$

In contrast to the DC-motor based IR template, whose dynamics were speed-dependent and displacement-independent, the piezo-based IR template takes the form of a forced, undamped harmonic oscillator.

III. ROBOT DESIGN AND FABRICATION

A. Morphology Design

In order to study the effects of inertial reorientation of a tail on an existing insect scale robot, we modified a Robofly created by Chukewad *et al*. The RoboFly [25], [2], [26] is a 74 mg flapping wing robot, designed and fabricated at the Autonomous Insect Robotics lab at the University of Washington. It is designed to operate through two flapping wings actuated by two independent piezoelectric bi-morph actuators. In its original configuration, one actuator points forward and the other aft, so that the mass is balanced about the wings.

For this work, we altered this basic design by adding an additional identical actuator unit between these two, mounted perpendicularly. This third actuator drives the tail (Fig. 1). We built two devices – a simple, wingless testbed to explore piezo-driven inertial reorientation and test our controller, and a flight-capable testbed for aerial experiments. The remainder of this section will discuss the body-centered tail testbed; for details of the flight prototype, see Sec. IV-D.

For our simplified device operating with template dynamics, we removed the wings and added a counterbalance sufficient to locate the center of mass at the tail joint (Fig. 2). To design the tail, we aimed to achieve an effectiveness of approximately 0.5 so the tail and body would move by equal amounts in opposite directions during reorientation (by (3)). The tail length l_t was chosen to be 15 mm, just long enough to avoid any obstruction to the wire tethers that attach to the actuator about 12 mm from the pivot. Since the body

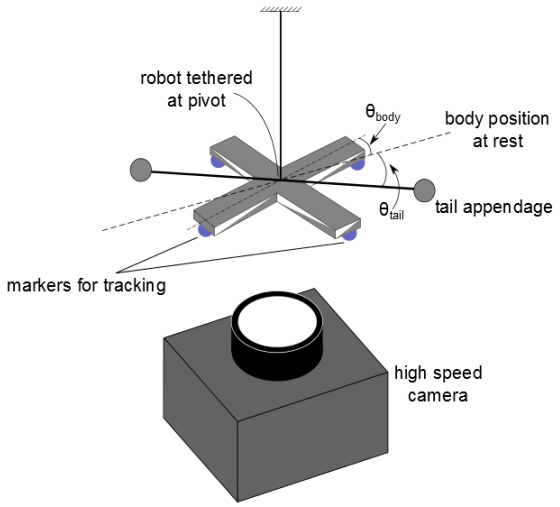

Fig. 4. Apparatus used for experiments on tethered physical testbed of template dynamics.

is composed of three radially-oriented actuators and one counterweight, we approximated the inertia about its CM, I_b, as approximately four times the inertia of a single actuator-airframe about its end (taken from a computer model in [27]). Using this value in the effectiveness equation, (2), we were able to compute an approximate desired tail inertia. Assuming the masses at the end of the tail act as point masses, we estimated their necessary mass m_t from

$$I_t = 2l_t^2 m_t,$$

neglecting the mass of the connecting carbon fiber rod, which weighed less than 3 mg. Length and mass of the tail can be found in Table I.

The maximum rotation of the body is the product of effectiveness and the total range of motion of the tail. For a given piezo actuator, the tail stroke is limited by the product of maximum safe voltage and the mechanical advantage of the transmission. Selection of transmission ratio ultimately entails a tradeoff between maximum body rotation (via tail range of motion) and speed of response (via available torque to accelerate the tail/body mass). For this testbed, we chose flexure geometry similar to that used for the wing hinges, which led to relatively small range of motion and rapid response. With a maximum safe voltage of 250 V (to avoid damage to the actuator), the full tail range of motion (from one extreme position to the other) was approximately 55° (see Fig. 7).

B. High-voltage piezo signal

We used a Simulink Real-Time (formerly xPC Target) (Mathworks, Natick, MA) and a data aquisition board with analog output capability (National Instruments model PCI-6259) to generate analog signals. These were amplified using a piezo amplifier (Trek model 2205).

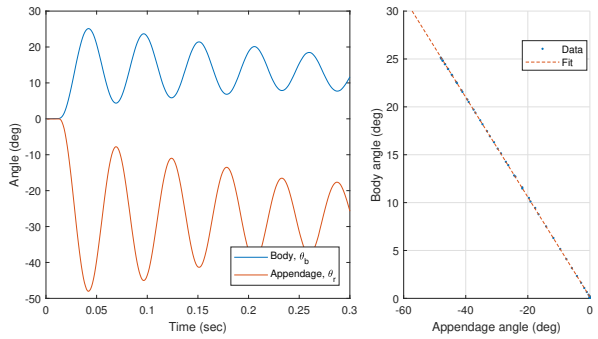

Fig. 5. Kinematic data from experiment used to identify effectiveness and inertia. (Left) Body and tail kinematics after a step input. (Right) Body angle θ_b regressed against tail angle θ_r.

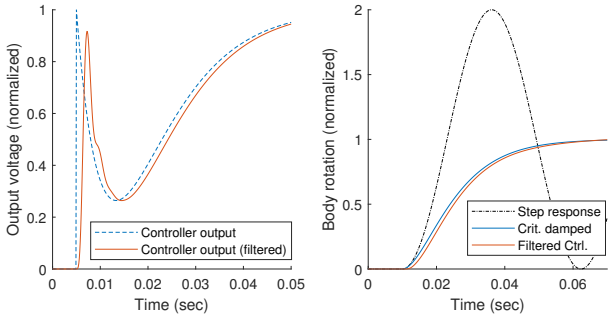

Fig. 6. Designed trajectory and model predictions. (Left) Signal output by the feedforward controller for critically damped reorientation before (blue) and after (red) lowpass filter to prevent actuator damage. (Right) Step response of body dynamics (5) compared to critically-damped reorientation using feedforward controller (raw and filtered).

C. Fabrication

The robot was fabricated with laser micromachining using a diode-pumped solid-state frequency tripled Nd:Yag laser with 355 nm wavelength (PhotoMachining, Inc.) and pin-aligned multilayer thermal sheet adhesion [28].

Our design departs from an earlier design [1] by creating the airframe from a single part rather than approximately 9 separate parts, simplifying fabrication. Using a single laminate sheet rather than discrete components also allows for features like castellated folds and mechanical locks. More details of the design and fabrication of the basic actuator can be found in [25].

D. Feedforward Controller Design

The robot's small size and payload limits currently preclude on-board sensing and feedback control of tail angle. Fortunately, the piezo actuator's spring-like mechanics greatly simplify control when compared to an idealized DC motor – quasistatically, the tail angle can be controlled in open loop by modulating voltage (e.g. when $\tau_a = 0$ in Eqn. 1). However, these same properties result in large, underdamped oscillations when the tail voltage is applied as a step (see Fig. 5), which would be transmitted to the body in equal proportion. To control inertial reorientation while minimizing unwanted vibration, we designed an open loop voltage waveform that avoids exciting the vibration mode.

Since the plant dynamics are linear and second order, one simple choice for target dynamics is a critically-damped oscillator driven by a proportional-derivative controller,

$$I_b\ddot{\theta}_b = \tau_b = K_P(\theta_{b,ref} - \theta_b) - K_D\dot{\theta}_b, \tag{6}$$

where τ_b is the total torque applied to the body, and for critical damping, $K_D = 2\zeta\sqrt{K_P I_b}$. For a step in $\theta_{b,ref}$, the critically-damped response is,

$$\theta_b(t) = \theta_{b,ref}(1 - e^{-\sqrt{K_P/I_b}t} - te^{-\sqrt{K_P/I_b}t}). \tag{7}$$

Because the actuator dynamics feature mechanical proportional feedback (i.e. spring torque), we let the proportional component of the torque be determined by the natural dynamics; matching terms in Eqn. 5, $K_P = K/\xi$. The time-varying voltage required to make the open-loop response track the critically-damped trajectory is,

$$V(t) = \frac{K\theta_{b,ref}}{\xi\rho} - \frac{K_D}{\rho}\dot{\theta}_b(t) \tag{8}$$

Differentiating (7) and plugging into (8) yields the open-loop signal we designed, as plotted in Fig. 6. Simulation results are plotted in Fig. 6. Intuitively, this open loop input varies the voltage to mimic the damping force needed to eliminate vibration. Another way to view this controller is as a prefilter on a step input whose zeros cancel the oscillatory poles of the system dynamics.

TABLE I

DESIGN PARAMETERS OF TAIL TEMPLATE INSECT SCALE ROBOT

Parameter	Value	Units
ρ	0.38×10^{-6}	$\mathrm{N\,m\,V^{-1}}$
ξ	0.52	(dimensionless)
K	98×10^{-6}	$\mathrm{N\,m\,rad^{-1}}$
I_b	12×10^{-9}	$\mathrm{kg\,m^2}$
m_t	22.8×10^{-6}	kg
l_t	15×10^{-3}	m
I_t	13×10^{-9}	$\mathrm{kg\,m^2}$

E. Filtering

The piezo actuators have a strong (40 dB) self-resonant mode near 1000 Hz [21]; input signals with frequency content that excites this mode can damage the brittle actuators. To avoid this, we passed all signals through a 5th order low-pass Butterworth filter that attenuated signals at 1000 Hz by 40 db. The filter introduced a 2 ms delay to peak voltage (Fig. 6, left), but had a negligible impact on vibration cancellation (see Fig. 6, right). We applied the same filter to all inputs used experimentally, including a step input for comparison to our method.

IV. EXPERIMENTAL RESULTS

We performed two types of experiments: first, to identify the model parameters needed to generate the open-loop

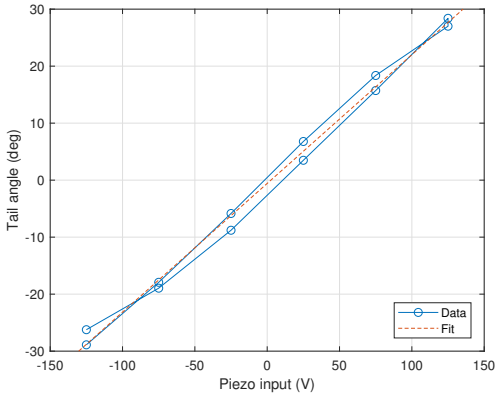

Fig. 7. Appendage movement as a function of piezo voltage at positive and negative 50 V increments. The difference between rising and falling curves is due to actuator hysteresis ($< 5\%$). The fit slope was used to estimate ρ.

voltage input, and second, to evaluate the performance of the open-loop trajectory.

Experiments on the flightless testbed were conducted on a tether. The robot was suspended by a Kevlar fiber attached near its pivot with the tail and body free to rotate in the horizontal plane. The Kevlar fiber's torsional stiffness was negligible, and we added weights to counter any unbalanced gravitational forces and minimize pendular behavior. The natural frequencies of all pendular modes associated with the tether were at least 10-fold higher than those of the body-tail behavior.

A. Estimation of Effectiveness and Body Inertia

We excited the body-tail system with a filtered step signal to collect vibration kinematics, which we used to estimate system parameters. Special markers were painted on the robot, and its motion was recorded using a high speed video camera (Vision Research Phantom v5.1). The video file was digitized using MATLAB and DLTv6 [29] and the discrete markers were tracked in each frame to measure the angles θ_b and θ_r.

Upon application of the step, the tail and body moved in opposite directions as expected (Fig. 5, left). The motion featured large, underdamped oscillations of body and tail. We estimated inertial effectiveness, ξ from kinematics using (3); ξ is the slope of the fit obtained from regressing θ_b on θ_r (Fig. 5, right). Our target effectiveness was $\xi = 0.5$; the actual measured value was approximately 4% higher. We updated our estimate of body inertia using the tail inertia and (2), assuming our tail inertia was more accurate, as it was generated by accurate measures of mass and length. Body parameters can be found in Table I.

B. Measuring Actuator Characteristics

We estimated torsional stiffness, K, from the natural frequency of the oscillations following a step input to the tail with the body grounded. We estimated the period, T, of the oscillations and thus the natural frequency, $\omega_0 = \frac{2\pi}{T}$, which we used to estimate actuator stiffness $K = \omega_0^2 I_t$.

We identified the torque-voltage calibration, ρ, by observing the variation of angle as voltage increased. We applied 50 V steps from zero to 250 V with the body grounded and measured tail angle. We repeated the experiment in both directions to estimate hysteresis (Fig. 7). As expected, displacement was approximately linear with voltage (Fig. 7). Hysteresis was under 5%, so we disregarded it in the sequel. We identified ρ from the slope using (1) with $\tau_a = 0$ (as the appendage was unloaded statically),

$$\theta_r = \frac{\rho}{K} V + \theta_{r0}, \tag{9}$$

where θ_{r0} is the rest angle of the appendage at zero voltage.

C. Reorientation behavior under feedforward control

Having identified the model parameters, we used the feedforward control approach to reorient the wingless robot in the tethered apparatus. As noted earlier, experiments in the tethered rig were subject to slow pendular dynamics which were excited by room air currents; the high speeds likely also generated small drag forces. These phenomena resulted in slow drifting behavior that we filtered out of the body angle before making measurements of performance.

We compared the performance of our feedforward controller to a step input (Fig. 8, center). The low damping of the piezo and transmission resulted in a step response characterized by large ($> 85\%$) overshoot and slow settling. By contrast, our feedforward "damped" controller exhibited relatively low overshoot (under 7%). While our goal was critically-damped behavior, it is unsurprising that some vibration remained, as model errors make perfect cancellation of plant dynamics impossible.

The performance of the inertial reorientation testbed was significant compared to state of the art for insect-sized robots. In the larger rotation, body angular velocity peaked at 1000 deg/sec about 7 ms from onset of movement (approximately one wingbeat period of the RoboFly), an angular acceleration of over 150,000 deg/sec^2. Our largest rotation was about 24 degrees in less than 35 ms, or about 5 wingbeats. However, these values should not be taken as a performance limit for a piezo-driven tail, as optimization of transmission geometry and refinements to increase effectiveness and decrease body inertia should be easily achievable relative to this simple testbed.

We tested linearity of our method by scaling the feedforward control by 50% and 150%, and measured body rotation 44% and 157%, respectively (Fig. 8, Right); the error corresponded closely to the hysteresis observed in the actuator and transmission. Better open-loop accuracy may be achieved with a more detailed hysteresis model. Nevertheless, our results demonstrate an ability to effectively servo the body using inertial reorientation with low overshoot using an open-loop controller.

D. Free Flight

We built a separate, flight-capable tailed RoboFly with design distinct from the tethered testbed. While the tethered testbed was designed for ease of analysis of piezo-driven

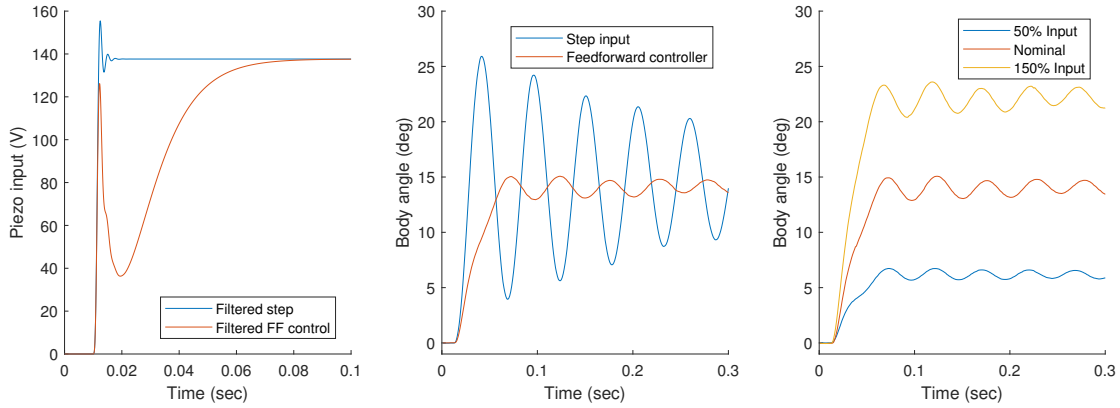

Fig. 8. Experimental results. (Left) Step and feedforward control inputs after low-pass filter. (Center) Resulting appendage behavior during inertial reorientation. Our controller decreases overshoot from roughly 85% to 7%. (Right) Scaling of voltage input. Modulating voltage resulted in nearly proportional modulation of body rotation.

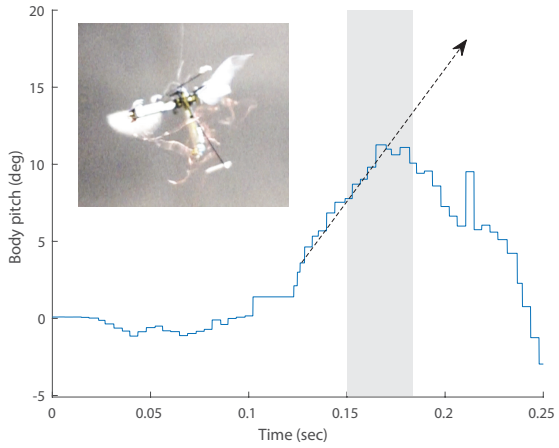

Fig. 9. Preliminary flight data from the tailed RoboFly. The robot took flight and maintained steady pitch for 20 ms before beginning to pitch back at roughly constant angular velocity (arrow indicates predicted trajectory). The tail was actuated at 150 ms (greyed region indicates period of tail motion), and pitch changes direction.

reorientation behavior, the flight prototype was designed to minimize tail mass. Tails with offset inertia (where the tail CM is not coincident with body CM) minimize mass per unit inertial effectiveness [5]. The tail of this system extends only downward. Its length was 15 mm and mass was 20 mg, giving an effectiveness of approximately half of the physical template. The added mass of the tail was primarily due to the additional actuator. Future designs should incorporate this mass in the actuated portion of the tail to increase effectiveness.

Preliminary data taken from a free flight in which the robot flew briefly before actuating its tail is shown in Fig. 9. The flight prototype took off about 100 ms into the trial and rose about 8 mm into the air, maintaining steady pitch for 20 ms before beginning to pitch back at roughly constant angular velocity. We actuated the tail 150 ms into the trial. The tail swing appeared to reverse the positive pitch velocity, and pitched the robot downward. Unlike the tethered robot's body-centered appendage, the tailed flight prototype's tail changes the location of the combined body-tail CM over its range of motion, likely modulating aerodynamic torque as well as generating inertial torque (as the CM moves relative to a body-fixed center of pressure (CP) from the wings). This additional torque could be controlled with the tail as a source of pitch control alternative to wing CP modulation.

V. CONCLUSIONS AND FUTURE WORK

In this report we described the modeling, analysis, design, and fabrication of an insect-sized robot with a piezo-actuated tail. It therefore departs from previous work in tail actuation that has exclusively been concerned with actuation by DC motor, providing for control of inertial torques at small scales. The open-loop stable appendage dynamics provided by the piezo in concert with our feedforward controller are a major advantage for miniaturized systems where feedback control remains a challenge. Our results demonstrate that inertial reorientation provides a possible avenue for extreme agility at this scale; we recorded significantly faster reorientations with our simple tail than the state-of-the-art for insect-sized vehicles. We anticipate potential utility of inertial forces for reorientation and stabilization of aerial vehicles, as well as miniaturized terrestrial vehicles such as HAMR [30].

This work forms the foundation for future small, piezo-actuated robots that must perform fast, dynamic maneuvers such as fast midair turns or precise pose alterations before landing. Future work will attempt to identify how to find mass and speed-optimal piezo and tail configurations, as was performed for DC motors in [6], and explore the use of inertial control in concert with aerodynamic control to maximize agility and robustness..

ACKNOWLEDGMENTS

This work partially supported by the Air Force Office of Scientific Research under grant no. FA9550-14-1-0398.

References

[1] K. Y. Ma, P. Chirarattananon, S. B. Fuller, and R. J. Wood, "Controlled flight of a biologically inspired, insect-scale robot," *Science*, vol. 340, no. 6132, pp. 603–607, 2013.

[2] J. James, V. Iyer, Y. Chukewad, S. Gollakota, and S. B. Fuller, "Liftoff of a 190 mg laser-powered aerial vehicle: The lightest wireless robot to fly," in *2018 IEEE International Conference on Robotics and Automation (ICRA)*, pp. 1–8, IEEE, 2018.

[3] P. Chirarattananon, K. Y. Ma, and R. J. Wood, "Fly on the wall," in *Biomedical Robotics and Biomechatronics (2014 5th IEEE RAS & EMBS International Conference on*, pp. 1001–1008, IEEE, 2014.

[4] S. Lupashin, A. Schöllig, M. Sherback, and R. D'Andrea, "A simple learning strategy for high-speed quadrocopter multi-flips," in *Robotics and Automation (ICRA), 2010 IEEE International Conference on*, pp. 1642–1648, IEEE, 2010.

[5] T. Libby, A. M. Johnson, E. Chang-Siu, R. J. Full, and D. E. Koditschek, "Comparative design, scaling, and control of appendages for inertial reorientation," *IEEE Transactions on Robotics*, vol. 32, no. 6, pp. 1380–1398, 2016.

[6] T. Libby, T. Y. Moore, E. Chang-Siu, D. Li, D. J. Cohen, A. Jusufi, and R. J. Full, "Tail-assisted pitch control in lizards, robots and dinosaurs," *Nature*, vol. 481, no. 7380, p. 181, 2012.

[7] N. Kohut, D. Haldane, D. Zarrouk, and R. Fearing, "Effect of inertial tail on yaw rate of 45 gram legged robot," in *Adaptive Mobile Robotics*, pp. 157–164, World Scientific, 2012.

[8] C. Casarez, I. Penskiy, and S. Bergbreiter, "Using an inertial tail for rapid turns on a miniature legged robot," in *Robotics and Automation (ICRA), 2013 IEEE International Conference on*, pp. 5469–5474, IEEE, 2013.

[9] A. Patel and M. Braae, "Rapid turning at high-speed: Inspirations from the cheetah's tail," in *Intelligent Robots and Systems (IROS), 2013 IEEE/RSJ International Conference on*, pp. 5506–5511, IEEE, 2013.

[10] U. Saranli, M. Buehler, and D. E. Koditschek, "Rhex: A simple and highly mobile hexapod robot," *The International Journal of Robotics Research*, vol. 20, no. 7, pp. 616–631, 2001.

[11] G.-H. Liu, H.-Y. Lin, H.-Y. Lin, S.-T. Chen, and P.-C. Lin, "A bio-inspired hopping kangaroo robot with an active tail," *Journal of Bionic Engineering*, vol. 11, no. 4, pp. 541–555, 2014.

[12] R. Briggs, J. Lee, M. Haberland, and S. Kim, "Tails in biomimetic design: Analysis, simulation, and experiment," in *Intelligent Robots and Systems (IROS), 2012 IEEE/RSJ International Conference on*, pp. 1473–1480, IEEE, 2012.

[13] J. Zhao, T. Zhao, N. Xi, M. W. Mutka, and L. Xiao, "Msu tailbot: Controlling aerial maneuver of a miniature-tailed jumping robot," *IEEE/ASME Transactions on Mechatronics*, vol. 20, no. 6, pp. 2903–2914, 2015.

[14] A. Demir, M. M. Ankarali, J. Dyhr, K. Morgansen, T. Daniel, and N. Cowan, "Inertial redirection of thrust forces for flight stabilization," in *Adaptive Mobile Robotics*, pp. 239–246, World Scientific, 2012.

[15] A. Jusufi, D. Kawano, T. Libby, and R. J. Full, "Righting and turning in mid-air using appendage inertia: reptile tails, analytical models and bio-inspired robots," *Bioinspiration & biomimetics*, vol. 5, no. 4, p. 045001, 2010.

[16] A. Jusufi, D. I. Goldman, S. Revzen, and R. J. Full, "Active tails enhance arboreal acrobatics in geckos," *Proceedings of the National Academy of Sciences*, vol. 105, no. 11, pp. 4215–4219, 2008.

[17] J. P. Dyhr, K. A. Morgansen, T. L. Daniel, and N. J. Cowan, "Flexible strategies for flight control: an active role for the abdomen," *Journal of Experimental Biology*, vol. 216, no. 9, pp. 1523–1536, 2013.

[18] J. P. Dyhr, N. J. Cowan, D. J. Colmenares, K. A. Morgansen, and T. L. Daniel, "Autostabilizing airframe articulation: Animal inspired air vehicle control," in *Decision and Control (CDC), 2012 IEEE 51st Annual Conference on*, pp. 3715–3720, IEEE, 2012.

[19] E. F. Helbling and R. J. Wood, "A review of propulsion, power, and control architectures for insect-scale flapping-wing vehicles," *Applied Mechanics Reviews*, vol. 70, no. 1, p. 010801, 2018.

[20] R. J. Wood, B. Finio, M. Karpelson, K. Ma, N. O. Pérez-Arancibia, P. S. Sreetharan, H. Tanaka, and J. P. Whitney, "Progress on picoair vehicles," *The International Journal of Robotics Research*, vol. 31, no. 11, pp. 1292–1302, 2012.

[21] B. M. Finio, N. O. Pérez-Arancibia, and R. J. Wood, "System identification and linear time-invariant modeling of an insect-sized flapping-wing micro air vehicle," in *Intelligent Robots and Systems (IROS), 2011 IEEE/RSJ International Conference on*, pp. 1107–1114, IEEE, 2011.

[22] B. F. Seitz, B. Goldberg, N. Doshi, O. Ozcan, D. L. Christensen, E. W. Hawkes, M. R. Cutkosky, and R. J. Wood, "Bio-inspired mechanisms for inclined locomotion in a legged insect-scale robot," in *2014 IEEE International Conference on Robotics and Biomimetics (ROBIO 2014)*, pp. 791–796, IEEE, 2014.

[23] M. H. Rosen, G. le Pivain, R. Sahai, N. T. Jafferis, and R. J. Wood, "Development of a 3.2 g untethered flapping-wing platform for flight energetics and control experiments," in *2016 IEEE International Conference on Robotics and Automation (ICRA)*, pp. 3227–3233, IEEE, 2016.

[24] R. Full and D. Koditschek, "Templates and anchors: neuromechanical hypotheses of legged locomotion on land," *Journal of Experimental Biology*, vol. 202, no. 23, pp. 3325–3332, 1999.

[25] Y. M. Chukewad, A. T. Singh, J. M. James, and S. B. Fuller, "A new robot fly design that is easier to fabricate and capable of flight and ground locomotion," in *2018 IEEE/RSJ International Conference on Intelligent Robots and Systems (IROS)*, pp. 4875–4882, IEEE, 2018.

[26] A. Singh, Y. Chukewad, and S. Fuller, "A robot fly design with a low center of gravity folded from a single laminate sheet," in *workshop on Folding in Robotics, IEEE conference on Intelligent Robots and Systems*, 2017.

[27] K. Y. Ma, S. M. Felton, and R. J. Wood, "Design, fabrication, and modeling of the split actuator microrobotic bee," in *Intelligent Robots and Systems (IROS), 2012 IEEE/RSJ International Conference on*, pp. 1133–1140, IEEE, 2012.

[28] J. P. Whitney, P. S. Sreetharan, K. Y. Ma, and R. J. Wood, "Pop-up book mems," *Journal of Micromechanics and Microengineering*, vol. 21, no. 11, p. 115021, 2011.

[29] T. L. Hedrick, "Software techniques for two-and three-dimensional kinematic measurements of biological and biomimetic systems," *Bioinspiration & biomimetics*, vol. 3, no. 3, p. 034001, 2008.

[30] A. T. Baisch, O. Ozcan, B. Goldberg, D. Ithier, and R. J. Wood, "High speed locomotion for a quadrupedal microrobot," *The International Journal of Robotics Research*, vol. 33, no. 8, pp. 1063–1082, 2014.